Interband Electronic Excitation–Assisted Atomic-Scale Restructuring of Metal Surfaces by Nanosecond Pulsed Laser Light

Hans-Joachim Ernst,* Fabrice Charra, Ludovic Douillard

Interaction of high-power laser light with materials often causes irreversible damage of the near-surface region. It is shown that copper single-crystal surfaces can be patterned by laser light. Irradiation with green light produced adatoms and vacancies, which self-organized into nanoscale pyramids. This restructuring can be removed by annealing. In contrast to green light, infrared laser irradiation at equivalent absorbed energy density did not produce any structural change. This, for metallic systems, unforeseen spectral difference in laser light action points to a concerted process as the source for structural modification, which involves long-lived primary excitation of localized d-electrons through interband transition together with phonon excitation.

The creation and dissipation of electronic excitation are fundamental for a variety of physical and chemical processes. Lasers, as a source of primary excitation, play an expanding role in material growth and processing and in photochemistry. However, the interaction of laser light with materials may also cause undesired effects, such as large-scale structural modification and damage of the near-surface region. In metallic systems, dissipation of electronic excitation into heat is normally very fast. Therefore, the structural change observed so far is damage, as the result of light-induced temperature rise that melts the material (*1*, *2*) or temperature rise–induced thermomechanical strain (*1*, *3*), which leads to plastic deformation through generation of bands of slip planes. Here, the coupling of a laser to atomic-scale structural probes such as helium atom beam scattering (HAS) and scanning tunneling microscopy (STM) provided the opportunity to discover that Cu surfaces can be nanostructured in a controlled manner by an electronic photo-physical process.

A Nd–yttrium-aluminum-garnet laser, operating at a wavelength (λ) of 532 nm (green light) or 1064 nm [infrared (IR) radiation] at a variable pulse repetition rate between 0.1 and 10 Hz, was linked to either the HAS apparatus or the STM, both operating at a base pressure of about 10^{-10} torr. In most experiments reported here, the laser provided light pulses with a temporal width of 10 ns in a "top hat" section profile 5.5 mm in diameter. We performed some experiments by focusing the beam to a spot of half this diameter to increase the incident laser power density, which was then maximal at 11 MW/cm^2 for green light and at 416 MW/cm^2 for IR radiation. Linearly polarized laser light reached the sample through a view port at nearly normal incidence, so that reflected light did not induce desorption of gas molecules from the inner walls of the vacuum system, which would have contaminated the sample. Also, plasmon excitation was not possible with this optical setup.

Our results were obtained on carefully polished, desulfurized Cu single-crystal surfaces spark cut within 0.2° to the (001) and (111) orientation. Before each laser experiment, we cleaned the surface at the atomic level by argon ion bombardment and removed the accompanying unwanted morphological disorder by annealing the surfaces to about 650 K for 20 min. This procedure resulted in a residual contamination level of the surface by oxygen and water of less than 0.5% of a monolayer and defect-free terrace sizes of about 800 Å on the average.

Photon absorption in metals occurs through interaction with electrons, raising them to higher energy levels within the conduction band. These transitions can be intraband or interband, depending on photon energy. The excited electrons relax for the most part not radiatively, but by electron-electron and electron-phonon collisions, heating up the electron system and finally the crystal lattice. In metallic systems, these collisional processes are complete within a few picoseconds (*4*). Thus, within the time scale of excitation with 10-ns laser pulses, optical energy is nearly instantaneously transformed into heat at the point at which the light is absorbed. Therefore, the system can be characterized by a temperature, and classical heat flow equations can be used to describe the time-dependent temperature profile at the surface resulting from the impinging laser pulse. For large-spot nanosecond laser beams directed onto metallic surfaces, the depth to which heat is conducted during the laser pulse is typically large (≈1 μm) as compared with the penetration depth of light (≈150 Å) but is much smaller than the size of the laser spot in the plane of the surface. Therefore, heat conduction can be described within a simple one-dimensional model (*5*) for which analytical solutions exist. These solutions have been shown to provide an accurate description of the light-induced temperature rise in metallic systems, including Cu (*5*). On the basis of these established formulas, we determined the peak transient temperature rise to about 115 K for the largest incident fluence of 114 mJ/cm^2 (at λ = 532 nm) applied in our experiment.

The hitherto observed irreversible damage is characterized by thresholds (*1*–*3*, *6*, *7*) in absorbed photon fluences that translate into thresholds in transient temperature rises, which are material dependent but independent of laser wavelength. In view of this so far commonly accepted picture of laser light–metal interaction, we should not see any structural modification at all (*1*) for the modest transient temperature rises applied. Also, Arrhenius-type thermal activation because of overall temperature rise (static temperature plus transient temperature rise, lasting only a few nanoseconds) of atomistic kinetic processes characterized by activation energy barriers (*8*), such as the creation of adatoms or desorption of atoms, is negligible within the static temperature range of 90 and about 300 K covered by our experiment.

Both the helium atom beam and the laser beam were directed toward the sample. A pristine Cu(111) surface seen by HAS at the chosen helium atom wavelength is a perfect mirror, giving rise to specular scattering only. Helium atoms, unlike x-rays, electrons, or neutrons, do not penetrate into the sample but probe the outermost atomic layer exclusively. Therefore, any atomic-scale structural defect of this mirror leads to a readily measurable decrease in intensity of the reflected helium beam (*9*). The normalized helium atom beam reflectivity from Cu(111) was measured as a function of time during green laser light exposure at a pulse repetition frequency of 0.1 Hz (Fig. 1). The signal decreased in a stepwise fashion every 10 s as a result of the action of each single laser pulse. The laser light thus produced cumulative distortion of the surface on the atomic scale, the nature of which was identified with both HAS and STM as light-induced production of adatom-vacancy pairs.

The HAS experiment was performed at a static sample temperature of 90 K, at

Commissariat à l'Energie Atomique Saclay, Direction des Sciences de la Matière, Département de Recherche sur l'Etat Condensé, les Atomes et les Molécules, SRSIM, 91191 Gif-sur-Yvette, France.

*To whom correspondence should be addressed. E-mail: Ernst@santamaria.saclay.cea.fr

which adatoms and vacancies are largely immobile on this surface and do not nucleate into islands. This allowed the precise determination of the quantum efficiency of the light-induced production of adatoms and vacancies from a quantitative analysis of the helium reflectivity curves. In the limit of small defect coverage, the decrease of the helium reflectivity can be modeled (9) by $I/I_0 = 1 - n\Sigma\Theta$, where n is the number density of atoms in the outermost atomic layer, Σ is the helium-defect cross section (the effective size of the defect as "seen" by the helium atom), Θ is the defect coverage, and I is the helium reflectivity with respect to the reflectivity I_0 of the pristine surface. Assuming a typical cross section Σ of 100 Å^2 for both adatoms and vacancies (9), we obtained an adatom-vacancy coverage of ≈1% of a monolayer from the decrease in helium reflectivity after the first laser shot. Knowing (*10*) the absorptivity A ($A = 1 - R$, where R is the light reflectivity) (λ = 532 nm) = 0.38, we inferred that at 114 mJ/cm^2 incident photon fluence, on average about 10,000 absorbed photons produce one adatom-vacancy pair in the outermost atomic layer of the surface.

The finding that green light interaction with Cu surfaces produces adatom-vacancy pairs was substantiated by our STM experiments, which were performed on a Cu(001) surface held at 300 K (Fig. 2). At this static temperature, light-generated adatoms and vacancies are mobile and nucleated into adatom and vacancy islands, respectively (Fig. 2A). The presence of vacancy islands excludes the possibility that adatoms were generated only by detachment from residual defects, such as steps, but implies instead that adatoms and vacancies were produced on terraces homogeneously in a concerted manner in the area illuminated by the laser beam. The STM topographs also illustrate that prolonged illumination led to the formation of nanoscale pyramids (Fig. 2B), similar to those found in the growth (*11*) of thin Cu films on Cu and in the exposure of Cu surfaces to argon ions (*12*). The origin of this phenomenon is traced back to an excess energy barrier for adatoms and vacancies to "vertical" diffusion [the Ehrlich-Schwöbel barrier (*13*)] associated with steps bordering islands. The light-induced nanostructuring can be reversed by heating the surface for a couple of minutes to 560 K, which completely restores the pristine surface.

Unexpectedly, the nanostructuring was found to be wavelength-dependent. When we tuned the laser wavelength to λ = 1064 nm (IR radiation, maximum peak transient temperature of about 105 K) at more than twice the equivalent absorbed photon fluence [on the basis of absorptivity (*10*) A (λ = 1064 nm) = 0.0095] for which adatom-vacancy production by green light is readily seen, no structural changes on Cu(001) or Cu(111) were observed. This lack of change was in evidence with STM and also HAS, in which no variation of the helium reflectivity during IR laser light irradiation was detected.

This surprising difference in laser action of green and IR light in a metallic system reveals that primary electronic excitation must play a key role in the production of adatoms and vacancies. The major difference in the excitation with IR and green light is that the latter is an interband excitation. Specifically, the strongly localized (*14*) Cu 3d electrons were excited a few tenths of an electron volt above the Fermi level in our experiment. How can this specific electronic excitation result in the formation of adatom-vacancy pairs?

The mechanism requires at first that the electronic excitation has a sufficiently long lifetime to couple to nuclear motion (about 100 fs is the typical time scale for a vibrational period). Moreover, on the basis of our observation that adatoms and vacancies are not produced at specific sites, such as residual defects, it requires an intrinsic process for the localization of energy, which then leads to the creation of adatoms and vacancies. Normally, these criteria are not fulfilled in metallic systems, where electronic excitations are short-lived and delocalized. However, a recent observation (*15*) might give a clue. Femtosecond photoemission studies of the electron dynamics on Cu surfaces reveal the presence of a long-lived (about 70 fs) exciton-like state, originating from the photoexcitation of Cu 3d electrons. This interband excitation generates a strongly localized 3d hole, which traps ex-

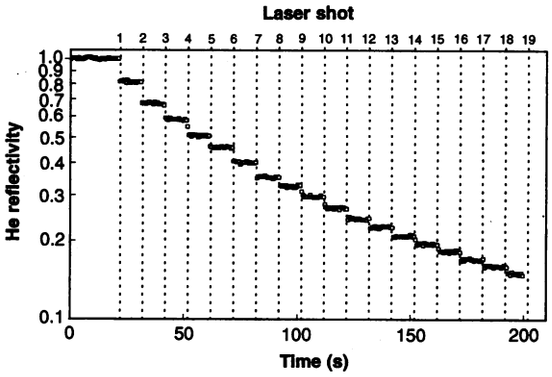

Fig. 1. Normalized helium atom beam reflectivity from Cu(111) held at a static temperature of 90 K under ultrahigh vacuum during laser action. The laser pulse repetition rate was set to 0.1 Hz: Synchronously with the laser shots, the helium reflectivity drops in a stepwise fashion because of green laser light–induced creation of adatoms and vacancies (see Fig. 2), which are immobile at this substrate temperature. Experimental parameters: Laser beam λ = 532 nm at 114 mJ/cm^2 fluence in 10 ns, linear polarization at normal incidence, and He atom beam wavelength λ = 0.58 Å.

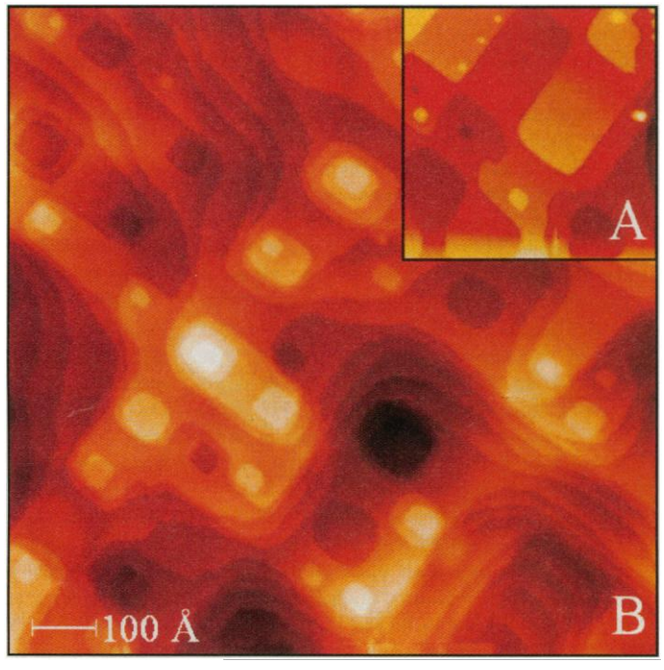

Fig. 2. Scanning tunneling microscope topographs (size 1000 Å × 1000 Å) from Cu(001) held at a static temperature of 300 K under ultrahigh vacuum, after (**A**) 12 laser shots and (**B**) 300 laser shots of green light. These images are representative of the area illuminated by the laser. At this substrate temperature, laser pulse–generated adatoms and vacancies are mobile and nucleate into both adatom and vacancy islands, respectively (A). Massive production of adatoms and vacancies after prolonged laser action leads to a restructuring in the form of nanoscale pyramids (B).

cited electrons through attractive Coulomb interaction. The spatial localization of these excited electrons reduces their probability for scattering with other electrons, resulting in longer lifetimes as compared with nonlocalized excited electrons. Just as in our experiment, in which structural modification was exclusively induced by the interband transition exciting green light, this long-lived electronic state is absent when intraband transitions by IR light are excited (*15*). We suggest that this long-lived excited electronic state induces a Jahn-Teller–like configurational distortion.

This long-lived electronic state cannot, however, be the only driving force. For an exclusively electronic origin, the rate of adatom and vacancy production should simply be proportional to the number of initially excited electrons, which in turn is proportional to the photon fluence (*16*), because nonlinear optical effects are excluded (*17*) in the fluence range covered by our experiment. We observed, however, that the production rate depended nonlinearly on fluence and, moreover, that it was enhanced at higher static sample temperatures. These findings suggest that phononic excitation also plays a role. Simultaneous adatom and vacancy production is characterized by an activation energy barrier (*8*), the height of which depends on the instantaneous configuration of the surrounding atoms. The probability that the minimal activation energy configuration is met increases with phononic excitation produced by static temperature and transient temperature rise. Thus, in this proposed picture, the concerted action of electronic and phononic driving forces leads to localization of energy and ultimately to the formation of an adatom-vacancy pair.

REFERENCES AND NOTES

1. A. M. Prokhorov, V. I. Konov, I. Ursu, I. N. Mihailescu, *Laser Heating of Metals* (Adam Hilger Series on Optics and Optoelectronics, Adam Hilger, Bristol, UK, 1990).
2. D. M. Follstaedt, S. T. Picraux, P. S. Peercy, W. R. Wampler, *Appl. Phys. Lett.* **39**, 327 (1981).
3. J. Frohn, J. Reynolds, T. Engel, *Surf. Sci.* **320**, 93 (1994); G. Hoogers, D. C. Papageorgopoulos, D. A. King, *ibid.* **310**, 147 (1994).
4. W. S. Fann, R. Storz, H. W. K. Tom, J. Bokor, *Phys. Rev. Lett.* **68**, 2834 (1992).
5. J. M. Hicks, in *Laser Spectroscopy and Photochemistry on Metal Surfaces*, H.-L. Dai and W. Ho, Eds., vol. 5 of *Advanced Series in Physical Chemistry* (World Scientific, Singapore, 1995), pp. 589–621.
6. H. M. Musal, "Laser induced damage in optical materials" (National Bureau of Standards Special Publication 568, Government Printing Office, Washington, DC, 1980), p. 159.
7. C. D. Marrs, W. N. Faith, J. H. Dancy, J. O. Porteus, *Appl. Opt.* **21**, 4063 (1992).
8. Z. Zhang and M. G. Lagally, *Science* **276**, 377 (1997).
9. B. Poelsema and G. Comsa, *Scattering of Thermal Energy Atoms from Disordered Surfaces*, vol. 115 of *Springer Tracts in Modern Physics* (Springer, Berlin, 1989).
10. J. Weaver, personal communication.
11. H.-J. Ernst, F. Fabre, R. Folkerts, J. Lapujoulade, *Phys. Rev. Lett.* **72**, 112 (1994); J.-K. Zuo and J. F. Wendelken, *ibid.* **78**, 2791 (1997).
12. H.-J. Ernst, *Surf. Sci. Lett.* **383**, L755 (1997).
13. G. Ehrlich and F. G. Hudda, *J. Chem. Phys.* **44**, 1039 (1966); R. L. Schwöbel, *J. Appl. Phys.* **40**, 614 (1969).
14. N. W. Ashcroft and N. D. Mermin, *Solid State Physics* (Holt, Rinehart, Winston, New York, 1976).
15. J. Cao, Y. Gao, R. J. D. Miller, H. E. Elsayed-Ali, D. A. Mantell, *Phys. Rev. B* **56**, 1099 (1997).
16. Y. Murata and K. Fukutani, in *Laser Spectroscopy and Photochemistry on Metal Surfaces*, H.-L. Dai and W. Ho, Eds., vol. 5 of *Advanced Series in Physical Chemistry* (World Scientific, Singapore, 1995), pp. 729–763.
17. T. A. Luce, W. Hübner, K. H. Bennemann, *Z. Phys. B* **102**, 223 (1997).

18. We thank J. Weaver for providing accurate and reliable experimental data for the absorptivity of Cu single crystals; P. Lavie and F. Merlet for technical assistance, P. Monchicourt for the loan of the laser system, and M. C. Desjonquères and D. Spanjaard for discussions.

22 September 1997; accepted 16 December 1997

The Origin of Chondrules at Jovian Resonances

S. J. Weidenschilling,* F. Marzari, L. L. Hood

Isotopic dating indicates that chondrules were produced a few million years after the solar nebula formed. This timing is incompatible with dynamical lifetimes of small particles in the nebula and short time scales for the formation of planetesimals. Temporal and dynamical constraints can be reconciled if chondrules were produced by heating of debris from disrupted first-generation planetesimals. Jovian resonances can excite planetesimal eccentricities enough to cause collisional disruption and melting of dust by bow shocks in the nebular gas. The ages of chondrules may indicate the times of Jupiter's formation and dissipation of gas from the asteroidal region.

Chondrules are millimeter-scale igneous silicate spherules that constitute as much as half of the mass of chondrites, the most common type of meteorite. Many sources for chondrules have been proposed (*1*), but there are problems with each mechanism (*2*). The preponderance of opinion (though far from unanimous) is that they were produced by transient heating events that melted primitive aggregates of dust within the solar nebula (*3*, *4*). Individual meteorites differ in mean compositions and sizes of their chondrules, implying that they were not mixed extensively in the solar nebula, but accreted into planetesimals soon after they solidified (*5*). However, many chondrules show evidence of multiple heating episodes, suggesting that heating events were localized and frequent (*6*).

The oldest components of chondrites are Ca-Al–rich inclusions (CAIs), millimeter- to centimeter-sized objects composed of refractory minerals. CAIs appear to have been exposed to high temperatures, possibly during the infall phase that formed the sun and the solar nebula (*7*). Some CAIs show evidence of in situ decay of ^{26}Al (half-life = 0.73 million years); those that lack such evidence appear to have been reprocessed (*8*). Unaltered and reprocessed CAIs can be found within the same meteorite, implying that alteration occurred before accretion. In contrast, few chondrules containing Al-bearing minerals show evidence for the presence of ^{26}Al at the time they solidified, implying that they formed a few million years later, after the ^{26}Al decayed (*9*).

Wood (*5*) suggested that chondrules were produced during the collapse that formed the solar nebula from the presolar cloud or during the accretion disk phase that redistributed the nebula's mass and angular momentum because more energy was released during these events than in the later, relatively quiescent nebula. Proposed early energy sources include infall of interstellar grain aggregates through an accretion shock (*10*); shock waves due to clumps of interstellar gas falling onto the disk (*11*); density waves in the disk (*12*); and outflows, jets, or flares from the early sun (*13*–*15*). The CAI-chondrule age difference, if real, argues against these mechanisms, which would have been effective during the first million years or less of the nebula's evolution. There have been numerous suggestions that chondrules were melted by shock waves in the nebula (*11*, *12*, *16*), but most mechanisms proposed for producing shock waves occur at the wrong time (too early to explain the CAI-chondrule age difference) or place (far from the nebula's central plane, or much closer to the sun than the present asteroid belt), or both.

It is generally assumed that CAIs and chondrules were produced before planetes-

S. J. Weidenschilling, Planetary Science Institute, Tucson, AZ 85705, USA.
F. Marzari, Dipartimento di Fisica, Universitá di Padova, 35131 Padova, Italy.
L. L. Hood, Lunar and Planetary Laboratory, University of Arizona, Tucson, AZ 85721, USA.

*To whom correspondence should be addressed. E-mail: sjw@psi.edu